

**Magnetoelastic coupling of compressively stressed Fe/GaAs(001)**

G. Wedler and B. Wassermann

*Institut für Experimentalphysik, Freie Universität Berlin, Arnimallee 14, D-14195 Berlin, Germany*

R. Koch

*Paul-Drude-Institut für Festkörperelektronik, Hausvogteiplatz 5-7, D-10117 Berlin, Germany*

(Received 12 March 2002; published 14 August 2002)

The magnetoelastic coupling, a property of major importance in heteroepitaxy, describes the dependence of the free energy of magnetic materials on strain and stress. Using our versatile UHV cantilever beam magnetometer we have investigated the magnetoelastic coupling constants  $B_1$  and  $B_2$  of Fe/GaAs(001), a system yielding compressed Fe(001) films. Both constants exhibit a strong dependence on the compressive film stress, which so far is not explained by theory: At stress values of about  $-0.5$  GPa the sign of  $B_1$  is positive and thus opposite to the bulk value;  $B_2$  is about 15% smaller than the bulk value.

DOI: 10.1103/PhysRevB.66.064415

PACS number(s): 75.70.-i, 75.80.+q, 68.60.Bs

**I. INTRODUCTION**

The magnetoelastic (ME) coupling interrelates the state of magnetization of ferromagnetic materials with lattice distortions. It is responsible for the well-known phenomenon of magnetostriction and can be quantified either via the ME coupling constants  $B_i$  (Ref. 1) or the magnetostriction constants  $\lambda_i$  (Ref. 2). For typical magnetostrictive distortions of  $10^{-3}$ – $10^{-5}$  the changes in the ME energy are negligibly small compared with the other magnetic contributions to the free energy. In heteroepitaxial thin films, however, intrinsic distortions due to lattice mismatch between film and substrate usually amount to a strain of several percent ( $\varepsilon \approx 10^{-2}$ ), thus affecting the ME energy substantially. It may even become comparable to the magnetocrystalline energy, which offers the challenging opportunity to stabilize new magnetic anisotropies different from the bulk<sup>3,4,5</sup> in heteroepitaxial thin films.

In the recent years it was convincingly shown by various experimental<sup>6–11</sup> and theoretical<sup>12–17</sup> studies that at strain values of a few percent a linear description of the ME energy ( $F_{\text{ME}} \sim B\varepsilon$ ) is no longer sufficient. It is convenient to use a series expansion in strain for the experimentally determined ME coupling constants  $B_i^{\text{expt}}$ :

$$B_i^{\text{expt}} = B_i + D_i\varepsilon + \dots \quad (1)$$

Here  $B_i$  is a ME coupling constant of the unstrained state, whereby good agreement with the corresponding bulk constants was found.<sup>7–9</sup>  $D_i$  is a second-order constant. In the case of Fe the second-order expansion of  $B_1$  is valid for a strain of at least  $\pm 4\%$  according to theoretical calculations.<sup>15</sup> Experimental studies, however, point to the necessity of third- or higher-order terms already at a tensile strain above  $+0.5\%$ ,<sup>9</sup> whereas films under compression have not been investigated so far.

In this study we report on the ME coupling constants  $B_1$  and  $B_2$  of Fe/GaAs(001), a technologically important heteroepitaxial system, where the influence of compressive strain on the ME coupling can be investigated. The misfit is  $-1.36\%$  ( $a_{\text{Fe}} = 0.2866$  nm,  $a_{\text{GaAs}}/2 = 0.2827$  nm); i.e.,

ideal coherent growth is accompanied by a compressive stress of  $-2.8$  GPa. Being one of the promising candidates for spin injection into semiconductors,<sup>18</sup> growth, epitaxy, and magnetism of Fe/GaAs(001) have been studied intensively in the past. It is well established that Fe grows epitaxially in its bcc modification with the (001) plane parallel to the substrate<sup>19</sup> both at elevated temperatures (420–450 K) (Refs. 20–22) and at room temperature (Refs. 23–26). However, due to diffusion of As and Ga into the Fe film, no sharp interface is formed.<sup>22,27,28</sup> Recent stress investigations<sup>29</sup> revealed that interdiffusion is reduced in films deposited at 300 K, but definitely not negligible.

**II. EXPERIMENT**

The experiments were performed in a multiple chamber UHV system (base pressure  $< 1 \times 10^{-10}$  mbar) equipped with a sensitive cantilever beam magnetometer (CBM) for *in situ* stress and magnetic measurements<sup>30</sup> and a four-grid low-energy electron diffraction (LEED) optics for *in situ* control of the substrate and film quality as well as a homebuilt UHV scanning tunneling microscope (STM) for *in situ* structural investigations. The substrates were cut from  $\approx 100$ - $\mu\text{m}$ -thick As-capped GaAs(001) wafers, which were prepared in a separate molecular beam epitaxy (MBE) chamber by removal of the oxide, deposition of an  $\approx 0.5$ - $\mu\text{m}$ -thick GaAs(001) buffer layer, and coating with a thin As layer. Prior to the Fe deposition the As capping layer was desorbed at about 650 K until (001) LEED spots were obtained; some of the substrates were additionally annealed for 1 h at 810 K, which exhibit also faint ( $2 \times 4$ ) and  $c(4 \times 4)$  superstructure spots. Fe was electron beam evaporated from a Knudsen-type tungsten source at a pressure better than  $2 \times 10^{-9}$  mbar; the deposition rate determined by a quartz crystal microbalance was  $0.008 \pm 0.001$  nm/s. Immediately after the film preparation the magnetic measurements were performed *in situ*. For the measurements of  $B_1$  the substrate orientation has to be chosen so that the [100] and [010] directions of the Fe(001) film are parallel to the length and width of the cantilever beam; the difference in magnetostrictive stress upon saturation magnetization along [100] and

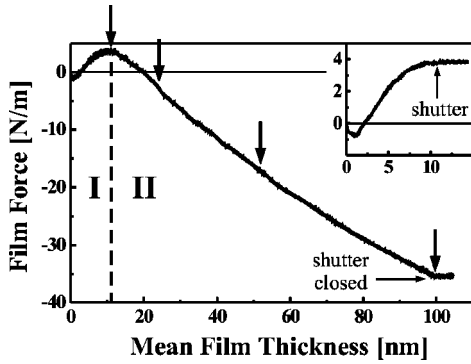


FIG. 1. Film forces (see text) measured in real time during the deposition of Fe onto GaAs(001) at 300 K; due to the biaxial in-plane stress distribution the stress behavior is isotropic. At the film thicknesses marked by arrows the magnetic properties, particularly the ME coupling constants were measured *in situ* with our cantilever beam magnetometer; notice that the force instantaneously remains constant when the shutter is closed (see, e.g., inset).

[010] then is equal to  $B_1$  ( $\sigma^{[100]} - \sigma^{[010]} = -B_1$ ).<sup>7,34</sup> For  $B_2$  the [110] direction of Fe(001) runs parallel to the long cantilever beam axis; saturation magnetization along [110] and [010] yields  $\sigma^{[110]} - \sigma^{[010]} = \frac{1}{2}B_2$ .<sup>9</sup>

### III. RESULTS

#### A. Stress of Fe/GaAs(001)

Figure 1 shows the film forces (integral forces in films of unit width) of Fe/GaAs(001) as a function of the average film thickness; they were measured in real time during the deposition of Fe onto an unannealed sample at 300 K. The overall stress behavior is in agreement with that of our recent study, where the involved stress mechanisms are discussed in full detail.<sup>29</sup> In short, after a compressive stress contribution due to changing surface stress at the very beginning (two to three monolayers) a tensile stress component dominates up to thickness of about 11 nm (regime I). This stress contribution is related to the restructuring of the interface proceeding when As and Ga atoms diffuse into the growing Fe film. At higher thicknesses eventually compressive stress owing to the lattice misfit is observed (regime II). Here the slope of the force curves corresponds to residual compressive stress of about  $-0.5$  GPa, indicating partial strain relief.

To facilitate the discussion of the ME coupling (see below) the following points should be elaborated in more detail here.

(i) The growth and stress behavior introduced above is typical for Fe/GaAs(001) at 300 K, both on annealed and on unannealed substrates. As discussed in Ref. 29 the tensile stress component is significantly increased on the unannealed, i.e., “As-richer,” samples and contributes up to a mean thickness of about 11 nm in the case of the Fe film of Fig. 1. It should be emphasized, however, that this does not necessarily mean that an 11-nm-thick layer is involved, but only that the tensile stress contribution becomes negligible after deposition of 11 nm of Fe. According to STM investigations by Bürgler *et al.*,<sup>31</sup> annealing of GaAs(001) sub-

strates close to the decomposition temperature—here at about 810 K—leads to a rough surface, where irregular hilllocks of about 1 nm height and several nm in diameter dominate the morphology. As indicated by Ref. 32 more gentle annealing after removal of the As cap generates a flatter surface exhibiting small As-rich ( $2 \times 4$ ) domains. The best surface configuration certainly is obtained with the *in situ*-prepared samples, where a fresh GaAs(001) layer is deposited directly after oxide removal.<sup>33</sup> Respective studies on such substrates could help to elucidate the influence of the surface corrugation (steps, domain boundaries, etc.) on intermixing. It should be pointed out, however, that the actual surface morphology of the GaAs(001) substrates is not relevant for the interpretation of the ME coupling of the compressively stressed Fe films presented here, because the contribution of the intermixed layer can be subtracted (see Sec. III C).

(ii) The occurrence of the tensile stress contribution is restricted to regime I; i.e., there is no further tensile stress contribution after passing the maximum of the force curve (marked by dashed line). This is confirmed by the force curve shown in the inset of Fig. 1, where the deposition has been stopped at 11 nm. Notice that the force stays constant immediately after the shutter has been closed. Also when the deposition is interrupted for the magnetic measurements at higher thicknesses (marked by arrows in Fig. 1) the force instantaneously remains constant. Since diffusion is a time-dependent process, the absence of a tensile force contribution after the deposition has been stopped verifies that interdiffusion effects are negligible above 11 nm.

(iii) As shown by x-ray absorption fine-structure spectroscopy<sup>35</sup> also in regime I the Fe lattice is compressed, but the total stress measured in regime I is dominated by tensile interface stress, which overcompensates the compressive misfit stress.

(iv) Arsenic is known to segregate to the surface.<sup>22</sup> The concentration of As in the bulk of thicker films, however, seems to be very small as indicated by recent x-ray photoelectron spectroscopy experiments;<sup>25</sup> after removing As from the surface by sputtering no further surface segregation was observed even after annealing at 200 °C.

#### B. Magnetization and anisotropy of Fe/GaAs(001)

The magnetic properties of Fe/GaAs(001) measured also *in situ* with our cantilever beam magnetometer are illustrated in Fig. 2 by means of 25-nm-thick Fe films; similar results were obtained with all investigated films between 11 nm and 100 nm. Figures 2(a) and 2(b) display hysteresis loops along the hard [110] and easy [100] axes, respectively. In accordance with previous studies<sup>23,24</sup> the experimental saturation magnetization lies between 1.7 and 1.9 MA/m. The good agreement with the Fe bulk value of 1.76 MA/m—within experimental error ( $\approx 10\%$ )—is indeed surprising and may indicate that the Fe thickness affected by intermixing is considerably smaller than 11 nm. Furthermore, all films exhibit the magnetic anisotropy of bcc-Fe with in-plane easy magnetization axes lying along [100] and [010]. This is con-

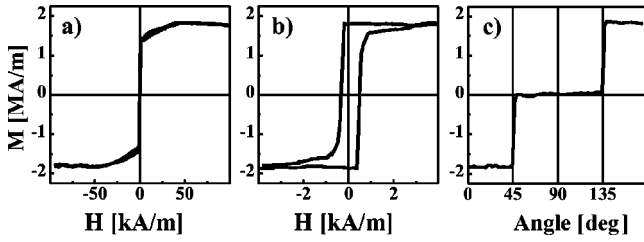


FIG. 2. Magnetic properties of 25-nm-thick Fe(001) films on GaAs(001): hysteresis loops (magnetization  $M$  vs magnetic field  $H$ ) (a) along the hard [110] axis and (b) along the easy [100] axis. (c) Dependence of the remnant magnetization along Fe[100] on the in-plane angle of the magnetizing field revealing easy axes along [100] and [010] (for details see text).

firmed by the anisotropy measurements, where the magnetizing field is rotated by 0-180° within the film plane. Figure 2(c) shows an example where the Fe[100] direction is parallel to the cantilever beam axis. The remnant magnetization component which in this case is measurable only along [100] is zero at field angles between 45° and 135°, because the remnant magnetization switches to the easy [010] direction when the magnetizing field is turned off.

### C. Magnetoelastic coupling of Fe/GaAs(001)

We investigated the ME coupling constants  $B_1$  and  $B_2$  of about ten different samples. We remark that particularly the measurement of  $B_1$  is an experimental challenge, because the 100- $\mu\text{m}$  thick GaAs(001) samples have to be cleaved along the difficult  $\langle 100 \rangle$  directions. Irrespective of the annealing treatment the measurements of both constants are quite reproducible. However, since the thickness of the intermixing region depends on the substrate preparation, we discuss the determination of the ME coupling constant  $B_1$  by means of the Fe film introduced in Fig. 1, where the deposition was interrupted for magnetic measurements at thicknesses of 11, 25, 50, and 100 nm.

In Table I, column  $B_1^{\text{expt}}$ , the experimental ME coupling constants measured in the  $B_1$  geometry are listed for Fe(001) films of various thicknesses (given in column  $t_F$ ). For all films  $B_1^{\text{expt}}$  differs decisively from the bulk value,  $B_1^{\text{bulk}} = -3.44 \text{ MJ/m}^3$ . It is opposite in sign, whereas the value of

TABLE I. ME coupling of Fe/GaAs(001) in  $B_1$  geometry:  $t_F$  is the film thickness,  $B_1^{\text{expt}}$  is the ME coupling constant as measured,  $B_1^{\text{II,eff}}$  is the effective ME coupling constant of the compressed Fe layer calculated by Eq. (2) with the 11 nm film as reference, and  $\sigma^{\text{II}}$  is the average stress of the compressed layer; bulk value of Fe:  $B_1^{\text{bulk}} = -3.44 \text{ MJ/m}^3$ .

$t_F$ [nm]	$B_1^{\text{expt}}$ [MJ/m <sup>3</sup> ]	$\sigma^{\text{II}}$ [GPa]	$B_1^{\text{II,eff}}$ [MJ/m <sup>3</sup> ]
11	+1.2	—	—
25	+2.5	-0.50	+3.5
50	+2.9	-0.49	+3.4
100	+2.9	-0.43	+3.1

the 11-nm-thick film, which is dominated by tensile stress (Fig. 1), is considerably lower.

As discussed above deviations of the ME coupling constants from the bulk value were frequently found for misfit-stressed heteroepitaxial films and attributed to nonlinear magnetoelasticity.  $B_1^{\text{expt}}$  of Fe films under tension, e.g., prepared on MgO(001) or W(001) substrates, differs significantly from the unstrained bulk value at stress values larger than 0.1 GPa, changes sign at about 0.7 GPa ( $\epsilon \approx 0.35\%$ ) and saturates after a steep linear increase at 2–3 GPa.<sup>7,8,9</sup> As intermixing can be excluded on MgO(001) and W(001), the films definitely are composed of pure Fe. In the case of Fe/GaAs(001), on the other hand, there is considerable diffusion of As and Ga into the growing film which may involve a layer with a thickness of about 11 nm as concluded from our stress results. Therefore caution is advised when trying to relate the observed deviations of  $B_1^{\text{expt}}$  of Fe/GaAs(001) with stress.

In order to separate the influence of intermixing we make use of the fact that the diffusion induced restructuring of the interface is restricted mainly to film thickness regime I. Accordingly, the experimental value  $B_1^{\text{expt}}$  is the sum of two contributions: the ME coupling of the film layer in regime I and the ME coupling of the compressively stressed layer in regime II. To extract the effective ME coupling constant  $B_1^{\text{II,eff}}$  of the compressively stressed layer from the experimental data, we subtract the ME coupling constant  $B_1^{\text{R}}$  of a reference film extending over regime I from  $B_1^{\text{expt}}$  (after normalization with respect to the film thickness)<sup>36</sup>:

$$B_1^{\text{II,eff}} = \frac{t_F}{t_F} B_1^{\text{expt}} - \frac{t_R}{t_F} B_1^{\text{R}}. \quad (2)$$

Here  $t_R$  denotes the thickness of the reference film and  $t_F$  the total film thickness. Note that both constants  $B_1^{\text{R}}$  and  $B_1^{\text{II,eff}}$  may still depend on strain [compare Eq. (1)] and  $B_1^{\text{R}}$  also on intermixing.

Column  $B_1^{\text{II,eff}}$  of Table I lists the effective ME coupling constants derived by Eq. (2) with the 11-nm-thick film as reference; in column  $\sigma^{\text{II}}$  the corresponding compressive stress determined from the average slope of the force curve in regime II is plotted. The extracted values of  $B_1^{\text{II,eff}}$  for the compressed Fe layers still are opposite in sign compared with bulk; moreover, they are even exceed  $B_1^{\text{expt}}$  and are the larger the larger  $\sigma^{\text{II}}$ .

Table II summarizes the respective results determined in the  $B_2$  geometry. For this sequence the reference film is 6 nm thick; we remind the reader that the thickness of regime I is influenced by the substrate preparation (see discussion in Sec. III A). Compared to  $B_1^{\text{II,eff}}$  the values of  $B_2^{\text{II,eff}}$  show a less dramatic dependence on the compressive stress. For  $\sigma^{\text{II}} \sim -0.5$  or  $-0.7$  GPa the values of  $B_2^{\text{II,eff}}$  are only slightly smaller than the bulk value ( $+7.62 \text{ MJ/m}^3$ ) and particularly have still the same sign.

Our experimental results on ME coupling and stress of Fe/GaAs(001) reveal that also compressive stress exerts strong influence on the ME coupling constants. At for heteroepitaxial systems still moderate stress values of about

TABLE II. ME coupling of Fe/GaAs(001) in  $B_2$  geometry:  $t_F$  is the film thickness,  $B_2^{\text{expt}}$  is the ME coupling constant as measured,  $B_2^{\text{II,eff}}$  is the effective ME coupling constant of the compressed Fe layer calculated by Eq. (2) with the 6 nm film as reference, and  $\sigma^{\text{II}}$  is the average stress of the compressed layer; bulk value of Fe:  $B_2^{\text{bulk}} = +7.62 \text{ MJ/m}^3$ .

$t_F$ [nm]	$B_2^{\text{expt}}$ [MJ/m <sup>3</sup> ]	$\sigma^{\text{II}}$ [GPa]	$B_2^{\text{II,eff}}$ [MJ/m <sup>3</sup> ]
6	+3.8	—	—
25	+6.4	-0.75	+7.2
25	+6.0	-0.53	+6.7

-0.5 GPa the sign of  $B_1$  is positive and thus opposite to the bulk value. The stress dependence of  $B_2$  is less pronounced, similar to the films under tension; at -0.5 GPa  $B_2$  is only about 15% smaller than the bulk value.

Can we understand this astonishing behavior of Fe under compressive strain? In recent *ab initio* calculations by Komelj and Fähnle,<sup>15</sup> based on the density functional theory, a parabolic dependence of the ME energy was found at least up to strain values of  $\pm 4\%$ . These results imply a linear dependence of  $B_1$  on strain, and thus the validity of a second-order expansion even for Fe films either compressed or expanded by  $\pm 4\%$ . In the case of Fe/MgO(001), however, we found a saturation of  $B_1$  (ca.  $+3.5 \text{ MJ/m}^3$ ) at a tensile strain of about 1.5% (2–3 GPa).<sup>9</sup> Obviously Eq. (1) with only second-order terms is not capable to correctly describe the experimental results and needs additionally terms of third (or higher) order. Also the positive values for  $B_1$  presented here for the compressed Fe films on GaAs(001) are not predicted by theory. Note that for a description based on second-order terms the magnitude of  $B_1$  increases linearly, when passing from tensile to compressive stress, which leads to larger negative values of  $B_1$  [see Eq. (1)] but not a reversal of sign. Therefore the second-order theory fails at consider-

ably lower strain values under compression—for  $\sigma \sim -0.5$ , i.e.,  $\varepsilon \sim -0.3\%$ , already positive values are observed—compared with Fe films under tensile strain ( $\varepsilon > 1.0\%$ ), which points to an asymmetry in the ME coupling under compression or tension. For the same arguments discussed above also the decrease of  $B_2$  at compressive strain is not in accordance with second-order ME theory.

#### IV. CONCLUSIONS

In conclusion, our parallel investigations of ME coupling, stress, and magnetic properties of Fe/GaAs(001) demonstrate that also at compressive stress the ME coupling constants deviate significantly from bulk. So far, however, not all experimental aspects of  $B_1$  and  $B_2$  are reproduced properly by theory, particularly concerning the change of sign in the case of  $B_1$  as well as the decrease of  $B_2$  of the compressively strained films. It appears, however, that there might be more severe problems inherent in the present *ab initio* density functional electron theory applied to Fe as even the correct sign of  $B_2$  for (unstrained) bulk Fe is not predicted correctly. As discussed in detail in Ref. 37 there seems to be a deficiency in the two approximations used commonly for the exchange-correlation functional, the local-spin-density approximation, and the generalized-gradient approximation. Nevertheless, the preliminary results presented here certainly need to be confirmed by future studies, where compressively strained epitaxial bcc Fe films are prepared on different substrates.

#### ACKNOWLEDGMENTS

We wish to thank M. Fähnle and G. Y. Guo for stimulating discussions, C. Pampuch for carefully reading the manuscript, K.-H. Rieder for his permanent support, and M. Höricke for providing the As-capped GaAs(001) substrates. The work was sponsored by the Deutsche Forschungsgemeinschaft (Sfb 290).

<sup>1</sup>Charles Kittel, Rev. Mod. Phys. **21**, 541 (1949).

<sup>2</sup>R. Becker and W. Döring, *Ferromagnetismus* (Springer-Verlag, Berlin, 1939).

<sup>3</sup>P. Bruno and J.-P. Renard, Appl. Phys. A: Solids Surf. **49**, 499 (1989).

<sup>4</sup>M. Farle, B. Mirwald-Schulz, A. N. Anisimov, W. Platow, and K. Baberschke, Phys. Rev. B **55**, 3708 (1997).

<sup>5</sup>G. Bochi, C. A. Ballentine, H. E. Inglefield, C. V. Thompson, and R. C. O'Handley, Phys. Rev. B **53**, R1729 (1996).

<sup>6</sup>R. C. O'Handley, Oh-Sung Song, and C. A. Ballentine, J. Appl. Phys. **74**, 6302 (1993).

<sup>7</sup>R. Koch, M. Weber, K. Thürmer, and K. H. Rieder, J. Magn. Magn. Mater. **159**, L11 (1996).

<sup>8</sup>A. Enders, D. Sander, and J. Kirschner, J. Appl. Phys. **85**, 5279 (1999).

<sup>9</sup>G. Wedler, J. Walz, A. Greuer, and R. Koch, Phys. Rev. B **60**, R11 313 (1999).

<sup>10</sup>D. Sander, Rep. Prog. Phys. **62**, 809 (1999).

<sup>11</sup>Th. Gutjahr-Löser, D. Sander, and J. Kirschner, J. Appl. Phys. **87**, 5920 (2000).

<sup>12</sup>R. Wu, L. Chen, and A. J. Freeman, J. Magn. Magn. Mater. **170**, 103 (1997).

<sup>13</sup>G. Y. Guo, D. J. Roberts, and G. A. Gehring, Phys. Rev. B **59**, 14 466 (1999).

<sup>14</sup>G. Y. Guo, J. Magn. Magn. Mater. **209**, 33 (2000).

<sup>15</sup>M. Komelj and M. Fähnle, J. Magn. Magn. Mater. **220**, L8 (2000).

<sup>16</sup>M. Komelj and M. Fähnle, J. Magn. Magn. Mater. **222**, L245 (2000).

<sup>17</sup>M. Komelj and M. Fähnle, J. Magn. Magn. Mater. **224**, L1 (2001).

<sup>18</sup>H. J. Zhu, M. Ramsteiner, H. Kostial, M. Wassermeier, H.-P. Schönherr, and K. H. Ploog, Phys. Rev. Lett. **87**, 016601 (2001).

<sup>19</sup>J. J. Krebs, B. T. Jonker, and G. A. Prinz, J. Appl. Phys. **61**, 2596 (1987).

- <sup>20</sup>M. Gester, C. Daboo, R. J. Hicken, S. J. Gray, A. Ercole, and J. A. C. Bland, *J. Appl. Phys.* **80**, 347 (1996).
- <sup>21</sup>P. M. Thibado, E. Kneedler, B. T. Jonker, B. R. Bennett, B. V. Shanabrook, and L. J. Whitman, *Phys. Rev. B* **53**, R10 481 (1996).
- <sup>22</sup>E. M. Kneedler, B. T. Jonker, P. M. Thibado, R. J. Wagner, B. V. Shanabrook, and L. J. Whitman, *Phys. Rev. B* **56**, 8163 (1997).
- <sup>23</sup>M. Zöphl, M. Brockmann, M. Köhler, S. Kreuzer, T. Schweinböck, S. Miethaner, F. Bensch, and G. Bayreuther, *J. Magn. Mater.* **175**, 16 (1997).
- <sup>24</sup>Y. B. Xu, E. T. M. Kernohan, D. J. Freeland, A. Ercole, M. Tselipi, and J. A. C. Bland, *Phys. Rev. B* **58**, 890 (1998).
- <sup>25</sup>T. L. Monchesky, B. Heinrich, R. Urban, K. Myrtle, M. Klaua, and J. Kirschner, *Phys. Rev. B* **60**, 10 242 (1999).
- <sup>26</sup>H.-P. Schönherr, R. Nötzel, W. Ma, and K. H. Ploog, *J. Appl. Phys.* **89**, 169 (2001).
- <sup>27</sup>S. A. Chambers, F. Xu, H. W. Chen, I. M. Vitomirov, S. B. Anderson, and J. H. Weaver, *Phys. Rev. B* **34**, 6605 (1986).
- <sup>28</sup>A. Filipe, A. Schuhl, and P. Galtier, *Appl. Phys. Lett.* **70**, 129 (1997).
- <sup>29</sup>G. Wedler, B. Wassermann, R. Nötzel, and R. Koch, *Appl. Phys. Lett.* **78**, 1270 (2001).
- <sup>30</sup>M. Weber, R. Koch, and K. H. Rieder, *Phys. Rev. Lett.* **73**, 1166 (1994).
- <sup>31</sup>D. E. Bürgler, C. M. Schmidt, J. A. Wolf, T. M. Schaub, and H.-J. Güntherodt, *Surf. Sci.* **366**, 295 (1996).
- <sup>32</sup>M. Fanfoni, E. Placidi, F. Arciprete, F. Patella, N. Motta, and A. Balzarotti, *Surf. Sci.* **445**, L17 (2000).
- <sup>33</sup>V. P. LaBella, H. Yang, D. W. Bullock, P. M. Thibado, P. Kratzer, and M. Scheffler, *Phys. Rev. Lett.* **83**, 2989 (1999).
- <sup>34</sup>P. M. Marcus, *Surf. Sci.* **366**, 219 (1996).
- <sup>35</sup>R. A. Gordon, E. D. Crozier, D.-T. Jiang, T. L. Monchesky, and B. Heinrich, *Phys. Rev. B* **62**, 2151 (2000).
- <sup>36</sup>Note that  $B_1^{\text{expt}}$  is calculated from the magnetostrictive stress  $\Delta\sigma_{\text{expt}} = \Delta F_{\text{expt}}/t_F = -B_1^{\text{expt}}$  with  $\Delta F_{\text{expt}}$  being the corresponding change of force measured by the CBM (see Ref. 7). Inserting  $\Delta F_{\text{expt}} = \Delta F_R + \Delta F_{\text{II}}$  with  $\Delta F_R/t_R = -B_1^R$  and  $\Delta F_{\text{II}}/t_{\text{II}} = -B_1^{\text{II,eff}}$  and using  $t_{\text{II}} = t_F - t_R$  one obtains Eq. (2).
- <sup>37</sup>M. Fähnle, M. Komelj, R. Q. Wu, and G. Y. Guo (unpublished).